Volume 18, Number 4, 2025. pp. 435-442

Jordan Journal of Physics

ARTICLE

Influence of Gas Flow Rate on the Plasma Temperature and Electron Density of an Atmospheric Argon Plasma Jet

Muna A. Issa[a,b] and **Kadhim A. Aadim**[a]

[a] *Department of Physics, College of Science, University of Baghdad, Iraq.*

[b] *Quality Assurance and Performance Evaluation Department, Mustansiriyah University, Baghdad, Iraq.*

Doi: **https://doi.org/10.47011/18.4.2**

Received on: 25/04/2024; *Accepted on: 16/10/2024*

Abstract: In this paper, an approach based on optical emission spectroscopy (OES) is used to experimentally determine the electron temperature (T_e) and electron number density (n_e) in an atmospheric argon (Ar) plasma jet. The Boltzmann plot method is applied to compute these parameters for gas flow rates ranging from 0.5 to 2.5 l/min. The results show the effect of gas flow rates on the plasma emission spectrum of argon (Ar I). Specifically, increasing the flow rate leads to an increase in the intensity of the spectral lines, particularly at 763.51 nm. Spectral lines of other molecules, such as N_2 and N_2^+, were also observed, showing the molecular interaction within the plasma. Strong OH and NO molecular emissions were detected, with OH emissions predominantly observed between 308 and 315 nm. Additionally, nitrogen molecular spectrum transitions were detected between 330 and 440 nm, including N_2^+ ions in the range of 391-436 nm. These results indicate that the gas flow rate is directly proportional to the emission intensity in the plasma, thus reflecting gas flow impacts on the plasma properties.

Keywords: Argon gas (Ar), Spectral characterization، Plasma temperature, Electron density, Plasma jet.

1. Introduction

Plasma is considered the fourth state of matter, alongside solid, liquid, and gas. It contains a collection of charged particles (ions and electrons) generated by heating a gas to an extremely high temperature or by exposing it to a very strong electromagnetic field, causing atomic ionization [1]. There are various production methods, including laser-induced plasma [2]. This method involves intense laser pulses focused on a material, causing it to ionize and form plasma. This technique is often used in fields like spectroscopy, material analysis, and fusion research. Unlike traditional plasma generation methods that require low-pressure environments, atmospheric pressure plasma operates at or near atmospheric pressure [3]. Dielectric barrier discharge plasma (DBD) [4] involves using an insulation material to generate plasma by applying an alternating electrical field across the material. This method is found in ozone generation, air purification, and thin-film deposition applications.

Cold atmospheric plasma (CAP) has been applied to modifying surfaces [5-7], producing nanoparticles from various materials. The combined effects of UV-radiation, moderate heat, and reactive types (such as oxygen-ROS and nitrogen-RNS) have often been recognized as the primary contributors to the antimicrobial activity of plasma. The impact of these distinct factors can fluctuate based on the parameters of the device [8]. Hydroxyl and oxygen groups are generated very efficiently in plasmas operating in atmospheric air and are identified regularly as

Corresponding Author: Muna A. Issa **Email**: muna.ahmed@sc.uobaghdad.edu.iq

crucial factors in the inactivation of germs. Therefore, this contributes greatly to the plasma's productivity. Devices operating in atmospheric air demonstrate notable efficiency in creating these agents. In recent times, cold atmospheric plasma (CAP) therapy has demonstrated considerable efficacy across a range of medical and biomedical applications [9-11], encompassing therapeutic, antimicrobial, and antineoplastic functions [12, 13]. This therapy is used due to its minimal cost, environmental friendliness, and lack of expensive equipment requirements.

Plasma diagnostics can be assessed by determining the electron temperature (T_e) and the electron density (n_e). Optical emission spectroscopy (OES) is the diagnostic method used for plasma analysis [14]. It takes a line devoid of self-absorption to determine n_e using the Stark broadening effect [15]. Self-absorption is a condition that can manifest itself in virtually any radiating system, including plasma. Furthermore, the plasma formation process in the air typically exhibits a significant temperature gradient due to the cooling effect of the ambient air [16]. In the outer regions of the cold plasma, elevated atom concentrations exist in lower energy states. Consequently, this situation could result in a noteworthy reabsorption of the emitted radiation lines [17]. A spectrograph and a detector are utilized to detect the plasma plume and achieve spectral resolution. The generated plasma spectrum can collect information regarding the elemental composition and various quantitative and qualitative data. The widths, variations, and shapes of the emission lines offer insights into the plasma's temperature and electron density. This research aims to understand how changes in the flow of argon gas affect the spectral emission intensity of argon and other molecular species present in the plasma. This contributes to a better understanding of plasma behavior and interactions within the atmospheric context.

2. Experimental Details

In the experimental setup, atmospheric cold plasma was generated utilizing a custom-built plasma jet system, as depicted in Fig. 1. A homemade DC power supply was employed, capable of generating high voltages up to a maximum of 13 kV at a frequency of 35 kHz. Within this setup, T_e and n_e were assessed across various gas flow-rate values.

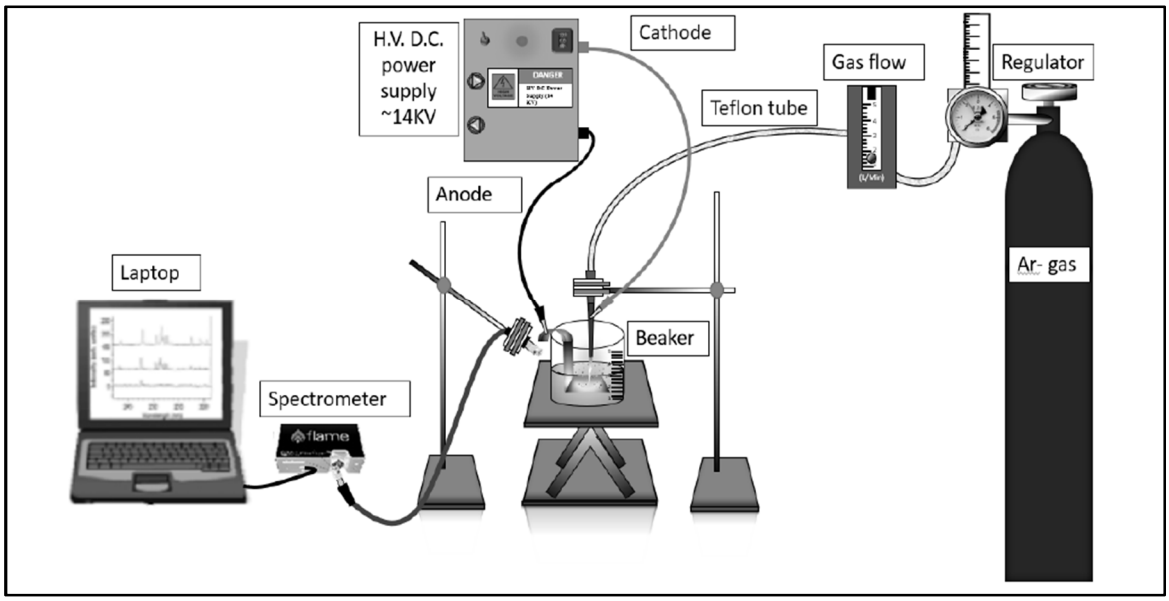

FIG. 1. DC plasma jet schematic with accompanying optical emission spectroscopic.

The configuration of the plasma jet was investigated in this work by detecting the excited species and their concentrations using the OES technique applied to discharges produced via an Ar plasma jet. Spectral data were recorded within the wavelength range of 160-1010 nm, directly from the jet of plasma in both radial and axial directions. To determine T_e (S3000-UV-NIR), as depicted in Fig. 2, a spectrometer was employed to collect and analyze the spectral data for this investigation.

FIG. 2. Spectrometer utilized in the experiment.

The spectrograph and detector are utilized to detect the plasma plume and achieve spectral resolution. Information regarding the elemental composition and various quantitative and qualitative data can be gleaned from the generated plasma spectrum. The emission lines' widths, variations, and shapes offer insights into plasma for n_e and temperature. Plasma temperature is a crucial thermodynamic property, as it characterizes and forecasts other plasma attributes, such as the distribution of energy level populations and particle speeds. In the laboratory experiment, the ratio method was utilized, assuming that the plasma maintains local thermodynamic equilibrium. The ratio method is a widely used approach for determining plasma temperature. It operates by comparing the intensity ratio of two spectral lines corresponding to transitions within the same ionization stage of an atom or ion. The plasma temperature (T) is determined using the following equation [18]:

$$T = \frac{(E_2 - E_1)}{k \ln(\frac{I_1 \lambda_1 A_2 g_2}{I_2 \lambda_2 A_1 g_1})} \quad (1)$$

where

- T: electron temperature to be calculated (in eV).
- E_1, E_2: energy levels of the molecules or atoms (in electron volts)
- k: Boltzmann constant (approximately 1.38×10^{-23} J/K).
- I_1, I_2: intensities of radiation at wavelengths λ_1 and λ_2, respectively.
- λ_1, λ_2: wavelengths of the radiation used (in nanometers).
- A_1, A_2: statistical weights or factors related to the transitions between energy levels 1 and 2.
- g_1, g_2: statistical weights for energy levels 1 and 2, reflecting the number of ways to distribute energy among the molecules.

Electron density refers to the quantity of free electrons within a given volume. The quadratic Stark effect obtained its name because the Stark broadening is proportional to the perturbing electric field. The electron density is subsequently calculated using the broadening parameters of the required spectrum [19]. The electric field, responsible for the impact of Stark in plasmas, is produced mainly by collisions with electrons. Consequently, it can be simplified to the following equation [20]:

$$n_e = \left[\frac{\Delta\lambda}{2\omega_s}\right] N_r \quad (2)$$

Here, ω_s is the theoretical line full-width Stark broadening parameter, calculated at the same reference electron density $N_r \approx 10^{17}\,cm^{-3}$.

3. Results and Discussion

In this experiment, the spectral lines were identified using databases such as the NIST Spectral Lines Database, a reliable reference that provides accurate information about the wavelengths and intensity of spectral lines for various elements, including argon. The spectral lines of argon (Ar I) and the weak lines of ionized argon (Ar II) were identified, and the values obtained were compared with those available in the NIST database to ensure the accuracy of the results [21]. The standard and the experimental values are illustrated in Tables 1 and 2, respectively.

TABLE 1. Standard values of argon gas from NIST.

Wavelength (nm)	$g_kA_{ki} \times 10^7$	E_i (eV)	E_j (eV)
696.5431	1.92	11.548354	13.327857
706.7218	1.90	11.548354	13.302227
763.5106	12.2	11.548354	13.171778
801.4786	4.64	11.548354	13.094872
811.5311	23.2	11.548354	13.075716

TABLE 2. Observed wavelengths and their intensities of argon gas at different flow rates.

0.5 (l/min)		1 (l/min)		1.5 (l/min)		2 (l/min)		2.5 (l/min)	
λ(nm)	Intensity (a u)	λ(nm)	Intensity (a u)	λ(nm)	Intensity (a u)	λ(nm)	Intensity (a u)	λ(nm)	Intensity (a u)
696.79	450.55	696.79	2768.85	696.79	3662.04	696.79	3637.17	696.30	4378.53
707.46	426.13	706.97	2876.11	707.46	3110.58	706.97	2871.67	706.97	2111.71
763.74	3094.30	763.74	17446.00	764.22	21778.00	764.22	22819.30	763.74	26709.20
801.58	1227.90	801.58	6002.00	801.58	8369.40	801.58	8182.70	801.09	9125.70
811.28	6125.74	810.79	32101.73	811.28	43784.43	811.77	42486.30	811.28	47241.10

Figure 3 exhibits the emission spectra of argon gas (Ar I) plasma under the influence of different gas flow rates. The spectrum intensity is plotted on the vertical axis, while the wavelength is shown in nanometers on the horizontal axis. It is clear from this figure that an increase in gas flow rate increases the spectral line intensities, especially those from argon (Ar I), indicating that the gas flow directly affects the properties of plasma and intensity of emission. The main spectral lines of argon (Ar I) can be seen in the wavelength scope of about 600 to 1000 nm. The most prominent of these lines is the one at 763.51 nm. Other notable emission lines occur at 750.39, 811.53, and 772.38 nm. These lines correspond to electronic transitions within argon atoms excited in the plasma. The spectral lines appear clearly at different flow rates but with greater intensity at higher flow rates, indicating the presence of higher n_e or greater electron energy, leading to an increase in these emissions [22].

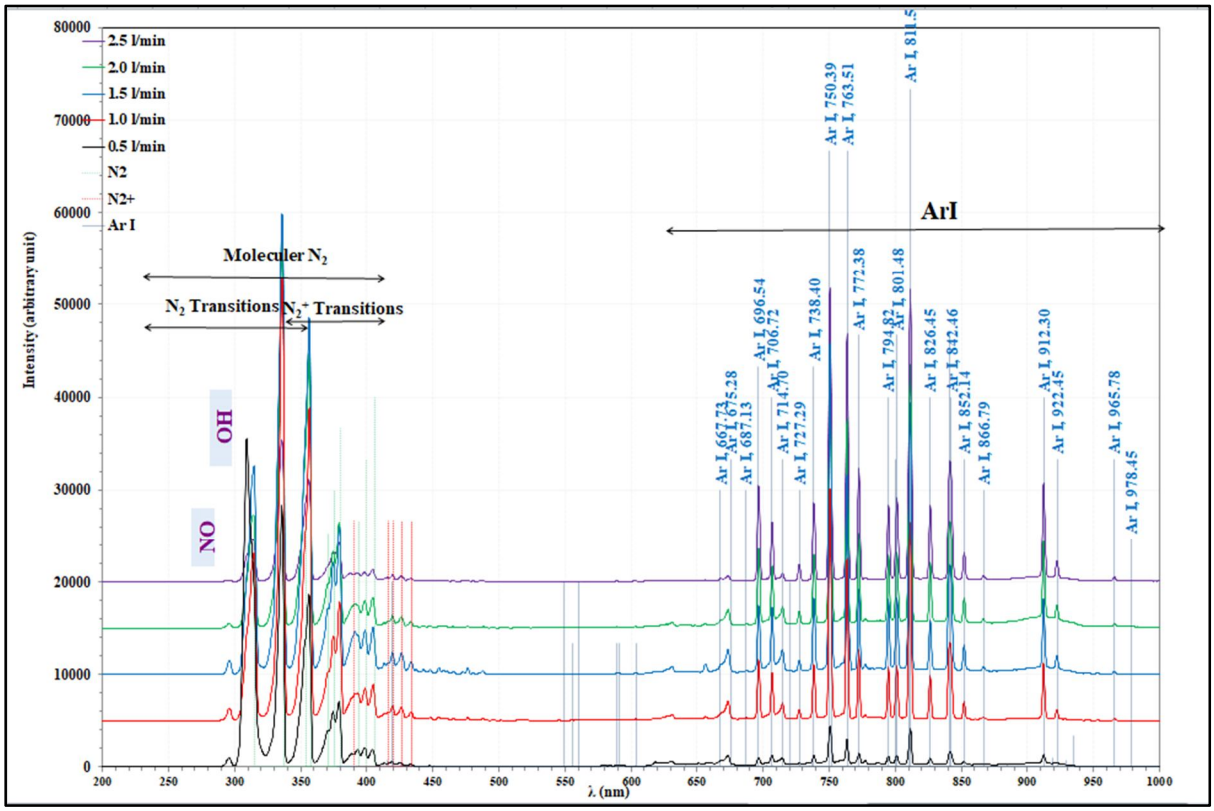

FIG. 3. Variation of intensity in terms of wavelength (nm) for diverse measurements of gas flow rate.

Molecular spectral lines of other gases, such as N_2 and N_2^+, can be observed in the wavelength region between 300 and 450 nm and are shown in Fig. 4 in more detail. These transitions express molecular interactions within the plasma, where argon, as a carrier gas, contributes to the excitation of these molecular species. Also appearing in this region are molecular lines of OH and NO molecules, which result from chemical reactions occurring within the plasma. The figure shows a significant variation in the intensity of these molecular lines depending on the gas flow rate, which illustrates the effect of different gas flow rates on the emission intensity. In the range between 308 and 315 nm, emissions of molecules such as OH and NO can be observed, which participate in chemical reactions within the plasma. Strong emissions characteristic of OH molecules appear at 308 nm. Several transitions of the molecular spectrum of nitrogen gas (N_2) have also been identified between 330 and 440 nm. These transitions are represented by the symbol Δv, which expresses the change in the quantum number of molecular vibrations. For example, in the spectral range around 357.69 nm, there are characteristic spectral lines of molecular nitrogen (N_2) with Δv = -1 and Δv = -2. This range also includes other transitions, such as Δv = 0 and Δv = -3, visible between 380 and 436 nm. In addition, molecular nitrogen ions (N_2^+) appear clearly in the region between 391 and 436 nm. Transitions in this range include ionic transitions that occur due to plasma excitation of nitrogen molecules, where an electron is lost from the molecule, resulting in the formation of ions that appear in the spectrum [23].

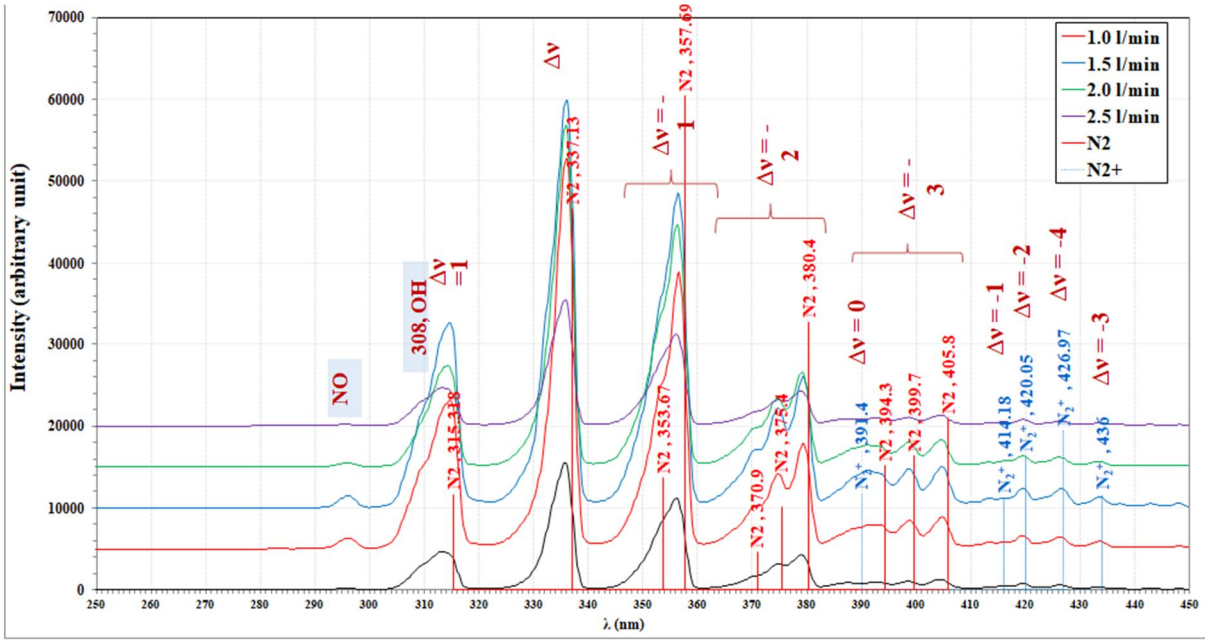

FIG. 4. Transitions of N_2.

The line at 763.51 nm was chosen because it is an isolated line that is not merged with other lines, has high intensity, and is apparent in all samples. Standard Stark coefficient values from previous studies are available for calculating n_e values. The highest peak observed in Fig. 5 demonstrates a noticeable trend: an increase in peak intensity corresponding to an increase in gas flow rate. This relationship suggests a direct correlation between the gas flow rate and the emission intensity within the plasma. As the gas flow rate rises, so does the emission intensity, indicating heightened emission activity within the plasma.

Electron temperature could be determined using Eq. (1), as illustrated in the corresponding curve in Fig. 6. Similarly, n_e can be obtained using Eq. (2).

There is less correlation in the five Boltzmann plots in Fig. 6; this is because the spectral lines chosen for these plots share the same energy level, making them particularly suitable for this study.

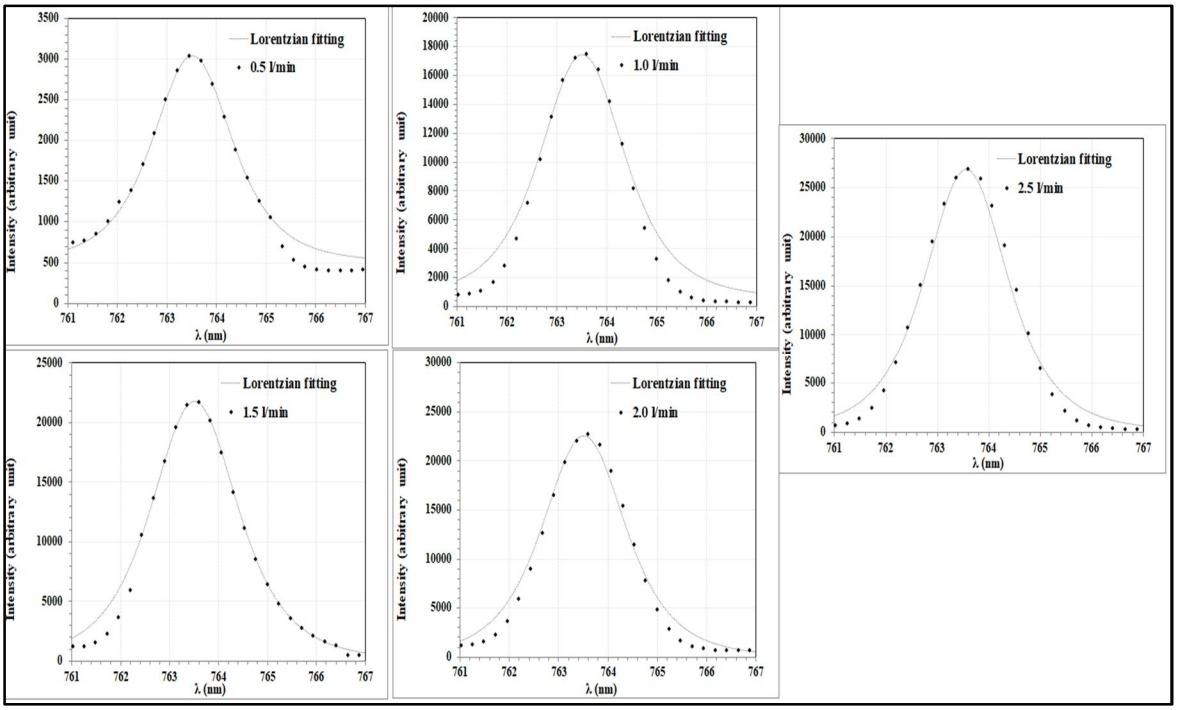

FIG. 5. Intensity variations in terms of wavelength (nm) at maximum peak for diverse gas flow rate measurements.

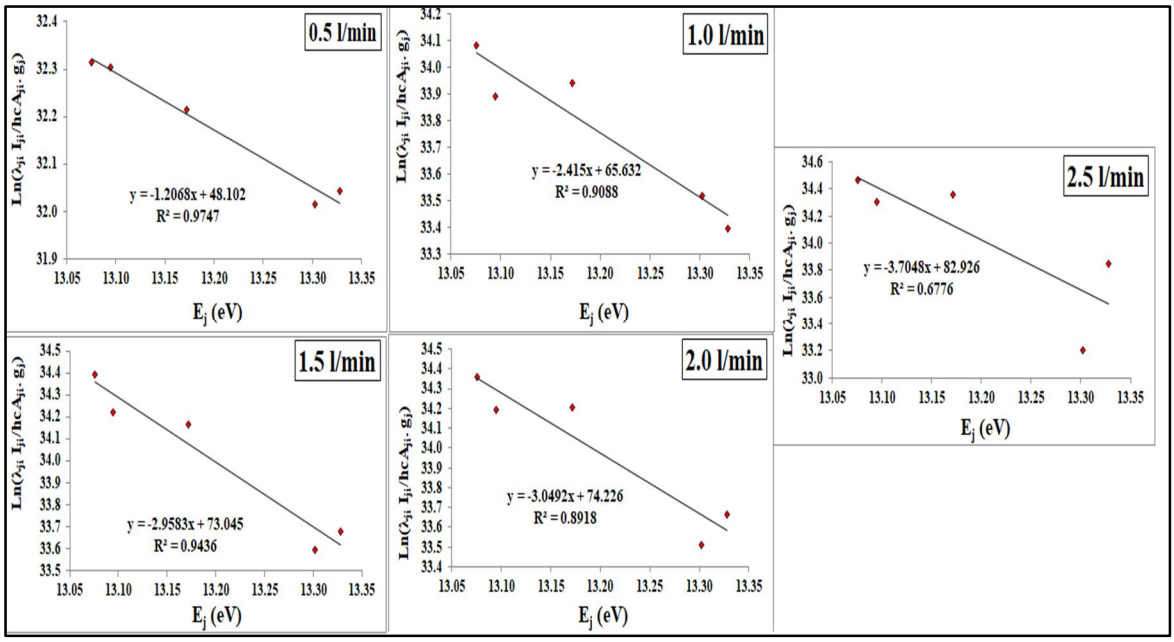

FIG. 6. Boltzmann plot for numerous gas flow rate values.

In Fig. 7, the association between n_e and T_e with respect to the gas flow rate is depicted. The figure illustrates a trend where T_e reduces as the gas flow rate ascends. Simultaneously, it demonstrates a contrasting trend where the plasma jet's electron density increases with the rise in gas flow rate. These findings align with previous observations reported by Aadim *et al.* [24, 25].

Indeed, an increased gas flow rate usually tends to increase the number of collisions between the gas atoms and plasma electrons. These collisions result in energy transfer from the electrons to the gas particles. The gas temperature ascends as this energy transfer intensifies due to increased collision frequency. Consequently, T_e decreases because a larger portion of the energy is transferred to the gas particles, thereby reducing the average energy level of the electrons within the plasma. Notably, these results align precisely with the results reported by Moon [26].

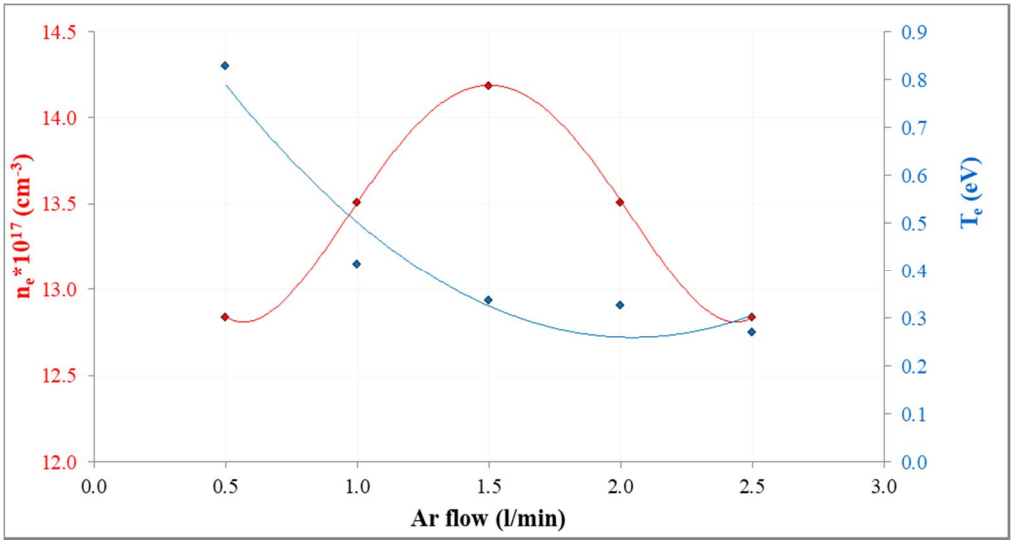

FIG. 7. Modification of T_e and n_e in terms of gas flow rate.

4. Conclusions

The presence of argon, reactive oxygen species, and reactive nitrogen in atmospheric pressure plasma was ascertained using optical emission spectroscopy. Furthermore, a correlation was observed between the gas flow rate, T_e, and n_e. Specifically, the gas flow rate exhibited a direct correlation with the electron density, while an increase in gas flow and plasma temperature demonstrated an inverse correlation.

5. Acknowledgments

This study is supported by the Plasma Physics Laboratory, Physics Department, College of Science, University of Baghdad.

References

[1] Palma, V., Cortese, M., Renda, S., Ruocco, C., Martino, M., and Meloni, E., Nanomaterials, 10 (8) (2020) 1596.

[2] Aadim, K.A., Opt. Quantum Electron., 48 (12) (2016) 545.

[3] Mazhir, S.N., Aadim, K.A., Al-Halbosiy, M.M.F., and Abdalameer, N.Kh., Indian J. Forensic Med. Toxicol., 15 (1) (2021) 2072.

[4] Abbas, I.K. and Aadim, K.A., Sci. Technol. Indones., 7 (4) (2022) 427.

[5] Ahmed, R.T., Ahmed, A.F., and Aadim, K.A., J. Opt. (India), 53 (2) (2024) 1564.

[6] Issa, M.A. and Aadim, K.A., J. Opt. (India), (2024). https://doi.org/10.1007/s12596-024-02212-2.

[7] Aadim, K.A., Photon. Sens., **7** (4) (2017) 289.

[8] Jamal, R.K., Ali, F.H., Hameed, M.M., and Aadim, K.A., Iraq. J. Sci., 61 (5) (2020) 1032.

[9] Weltmann, K.D. and Von Woedtke, T., Eur. Phys. J. Appl. Phys., 55 (1) (2011) 13807.

[10] Issa, M.A., and Aadim, K.A., J. Opt. (India), (2024). https://doi.org/10.1007/s12596-024-02034-2.

[11] Issa, M.A., and Aadim, K.A., J. Opt.(India), (2024). https://doi.org/10.1007/s12596-024-01951-6.

[12] Elahi, Z., Mahmood, S., and Zakaullah, M., Pak. J. Sci. Ind. Res. Ser. A: Phys. Sci., 66 (2) (2023) 130.

[13] Kostov, K.G., Rocha, V., Koga-Ito, C.Y., Matos, B.M., Algatti, M.A., Honda, R.Y., ... and Mota, R.P., Surf. Coat. Technol., 204 (18-19) (2010) 2954.

[14] Bates, D.R. and Bederson, B., "Advances in Atomic and Molecular Physics", (Academic Press, 1985).

[15] Evdokimov, K.E., Konischev, M.E., Pichugin, V.F., and Sun, Z., Resour.-Eff. Technol., 3 (2) (2017) 187.

[16] Rachdi, L., Sushkov, V., and Hofmann, M., Spectrochim. Acta B, 194 (2022) 106432.

[17] Amamou, H., Bois, A., Ferhat, B., Redon, R., Rossetto, B., and Matheron, P., J. Quant. Spectrosc. Radiat. Transfer, 75 (6) (2002) 747.

[18] Eggers, B., Marciniak, J., Memmert, S., Kramer, F.J., Deschner, J., and Nokhbehsaim, M., Odontology, 108 (2020) 607.

[19] Imran, H.J., Hubeatir, K.A., Aadim, K.A., and Abd, D.S., J. Phys.: Conf. Ser., 1818 (1, (2021) 012127.

[20] Jha, V.K., Mishra, L.N., and Narayan, B., Pak. J. Sci. Ind. Res. Ser. A: Phys. Sci., 66 (3) (2023) 261.

[21] Sansonetti, J.E., Martin, W.C., and Young, S.L., "Handbook of Basic Atomic Spectroscopic Data", (version 1.1. 2) (2005).

[22] Dwech, M.H., Aadim, K.A., and Hamid, L.A., AIP Conf. Proc., 2213 (2020) 020147.

[23] Kukhta, A.V. and Kazakov, S.M., Phys. Usp., 66 (2023) 173.

[24] Mohammed, R.S., Aadim, K.A., and Ahmed, K.A., AIP Conf. Proc., 2386 (2022) 080050.

[25] Ahmed, K.A., Aadim, K.A., and Mohammed, R.S., AIP Conf. Proc., 2372 (2021) 080004.

[26] Moon, S.Y., Phys. Plasmas, 9 (3) (2002) 4045.